Design and realization of an all-fiber broadband tunable gain equalization filter for DWDM signals

R. K. Varshney[1] and B. Nagaraju[1], A. Singh[1,2], B. P. Pal[1,3]and A. K. Kar[4,*]

[1]*Physics Department, Indian Institute of Technology Delhi*

New Delhi 110 016, India
ravi@physics.iitd.ac.in, bppal@physics.iitd.ac.in
[2]*Present address: ECSE Department, Monash University*
Clayton 3800, Melbourne, Victoria, Australia
[3]*Erasmus Mundas Visiting Scholar at Heriot-Watt University on sabbatical leave from IIT Delhi*
[4]*School of Engineering and Physical Sciences, David Brewster Building, Heriot-Watt University*
Edinburgh EH14 4AS, Scotland, United Kingdom
[*]*Corresponding author: a.k.kar@hw.ac.uk*

Abstract: Design and fabrication of a tunable gain equalization filter for dense wavelength division multiplexed (DWDM) signals through erbium doped fiber amplifiers (EDFA) is reported. It is based on a side-polished fiber (SPF) half-coupler block loaded with a displaceable tapered multimode overlay waveguide (MMOW). A simple and accurate normal mode analysis is employed to design this filtering device for its subsequent realization. Equalization of a typical EDFA gain spectrum in the C-band within ±0.35 dB or even less in the presence of various ITU standard C-band DWDM signal channels is demonstrated under varied operating conditions like add/drop of signals. Tunability of the filter notch is achieved through displacement of the SPF relative to the MMOW.

OCIS codes: (060.0060) Fiber optics and optical communications; (060.2310) Fiber optics; (060.2340) Fiber optics components; (060.2410) Fibers, erbium; (230.7408) Wavelength filtering devices

References and links

1. A. Srivastava and Y. Sun, Chapter 12 "Erbium doped fiber amplifiers for dynamic optical networks," in *Guided wave optical components and devices: basics, technology and applications*, B.P. Pal., ed. (Academic Press, Elsevier, Burlington, 2006), pp. 181-203
2. C.G. Atkins, J.F. Massicott, J.R. Armitage, R. Wyatt, B.J. Ainslie, and S.P. Craig-Ryan, "High-gain, broad spectral bandwidth erbium-doped fiber amplifier pumped near 1.5 µm," Electron. Lett. **25**, 910-911 (1989).
3. S. Yoshida, S. Kuwano, and K. Iwashita, "Gain-flattened EDFA with high Al concentration for multistage repeatered WDM transmission systems," Electron. Lett. **31**, 1765-1767 (1995).
4. A. Mori, Y. Ohishi, M. Yamada, H. Ono, Y. Nishida, K. Oikawa, and S. Sudo, "1.5 µm broadband amplification by tellurite-based EDFA's," in *Optical Fiber Communication conference*, Technical Digest (Optical Society of America, 1997), post-deadline paper PD1.
5. M. Yamada, H. Ono, A. Mori, T. Kanamori, S. Sudo, and Y. Ohishi, "Ultra-broadband and gain-flattened EDFA's for WDM signals," in *Optical Amplifiers and Their Applications*, Technical Digest (Optical Society of America, 1997), paper MB1.
6. M. Yamada, A. Mori, K. Kobayashi, H. Ono, T. Kanamori, K. Oikawa, Y. Nishida, and Y. Ohishi, "Gain-Flattened Tellurite-Based EDFA with a Flat Amplification Bandwidth of 76 nm," IEEE Photon. Technol. Lett. **10**, 1244-1246 (1998).
7. J. Y. Pan, M. A. Ali, A. F. Elrefaie, and R. E.Wagner, "Multiwavelength fiber-amplifier cascades with equalization employing Mach-Zehnder optical filter," IEEE Photon. Technol. Lett. **7**, 1501-1503 (1995).
8. H.S. Kim, S.H. Yun, H. K. Kim, N. Park, and B.Y. Kim, "Actively Gain-flattened erbium-doped fiber amplifier over 35 nm by using all-fiber acousto-optic tunable filters," IEEE Photon. Technol. Lett. **10**, 790 - 792 (1998).
9. B.Y. Kim, S.H. Yun, and B.W. Lee, "Acousto-optic filter", US Patent No. 6,532,323 B2 (2003).

#86448 - $15.00 USD Received 13 Aug 2007; revised 24 Sep 2007; accepted 24 Sep 2007; published 1 Oct 2007

10. S. Li, K. S. Chiang, and W. A. Gambling, "Gain flattening of an erbium doped fiber amplifier using a high-birefringence fiber loop mirror," IEEE Photon. Technol. Lett. **13**, 942–944 (2001).
11. N. Kumar, M.R. Shenoy, and B.P. Pal, "A standard fiber-based loop mirror as a gain-flattening filter for erbium-doped fiber amplifiers," IEEE Photon. Technol. Lett. **17**, 2056-2058 (2005).
12. M. Lelic, G.J. Cowley, and N. Menon, "Dynamic controller for a multichannel optical amplifier," US Patent No. 6,535,330 (2003).
13. R. Kashyap, R. Wyatt, and P.F. McKee, "Wavelength flattened saturated erbium amplifier using multiple side-tap Bragg gratings," Electron. Lett. **29**, 1025-1026 (1993).
14. C.R. Giles, "Lightwave applications of fiber Bragg gratings," IEEE J. Lightwave Technol. **15**, 1391-1404 (1997).
15. J-C. Dung, S. Chi, and S. Wen, "Gain flattening of erbium-doped fiber amplifier using fiber Bragg gratings," Electron. Lett. **34**, 555-556 (1998).
16. A. M. Vengsarkar, P. J. Lemaire, J. B. Judkins, V. Bhatia, T. Erdogan, and J. E. Sipe, "Long-period fiber gratings as band-rejection filters," IEEE J. Lightwave Technol. **14**, 58–64 (1996).
17. J.R. Qian and H.F. Chen, "Gain flattening fiber filters using phase shifted long period fiber gratings," Electron. Lett. **34**, 1132–1133 (1998).
18. Y. Liu, J.A.R. Williams, L. Zhang, and I. Bennion, "Phase shifted and cascaded long-period fiber gratings," Opt. Commun. **164**, 27–31 (1999).
19. P.D. Greene and H.N. Rourke, "Tailoring long period optical fiber gratings for flattening EDFA gain spectra," Electron. Lett. **35**, 1373-1374 (1999).
20. M. Harumoto, M. Shigehara, and H. Suganuma, "Gain-flattening filter using long-period fiber gratings," IEEE J. Lightwave Technol. **20**, 1027-1033 (2002).
21. Y.J. Rao, A.Z. Hu, and Y.C. Niu, "A novel dynamic LPFG gain equalizer written in a bend-insensitive fiber," Opt. Commun. **244**, 137 -140 (2005).
22. J.K. Bae, J. Bae, S.H. Kim, N. Park, and S.B. Lee, "Dynamic EDFA gain-flattening filter using two LPFGs with divided coil heaters," IEEE Photon. Technol. Lett. **17**, 1226-1228 (2005).
23. M.K. Pandit, K.S. Chiang, Z.H. Chen, and S.P. Li, "Tunable Long-Period Fiber Gratings for EDFA gain and ASE equalization," Microwave and Opt. Technol. Lett. **25**, 181-184 (2000).
24. I.B. Sohn, J.G. Baek, N.K. Lee, H.W. Kwon, and J.W. Song, "Gain flattened and improved EDFA using microbending long-period fiber gratings," Electron. Lett. **38**, 1324-325 (2002).
25. R.A. Bergh, G. Kotler, and H.J. Shaw, "Single-mode fiber optic directional coupler," Electron. Lett. **16**, 260-261 (1980).
26. C.A. Millar, M. C. Brierley, and S.R. Mallinson, "Exposed-core single-mode-fiber channel-dropping filter using a high-index overlay waveguide," Opt. Lett. **12**, 284-286 (1987).
27. D.G. Moodie and W. Johnstone, "Wavelength tunability of components based on the evanescent coupling from a side-polished fiber to a high-index-overlay waveguide," Opt. Lett. **18**, 1025 - 1027 (1993).
28. W.V. Sorin, "Broadband tunable in-line filter for fiber optics," US Patent no. 4.986,623 (1991).
29. R.B. Charters, A.P. Kuczyhski, S.E. Stakes, R.P. Tatam, and G.J. Ashwell, "In-line fiber optic channel dropping filter using Langmuir-Blodgett films," Electron. Lett. **30**, 594-595 (1994).
30. R. D. Pechstedt and P. St. J. Russell, "Narrow-band in-line fiber filter using surface-guided Bloch modes supported by dielectric multilayer stacks," IEEE J. Lightwave Technol. **14**, 1541-1545 (1996).
31. S. Zhao and B. Pi, "Mach-Zehnder interferometers and applications based on evanescent couplings through side-polished fiber coupling ports," US Patent no. 6,501,875 B2, (2002).
32. K. McCallion, W. Johnstone, and G. Fawcett, "Tunable fiber optic in-line bandpass filter," Opt. Lett. **19**, 542-544 (1994).
33. B.P. Pal, G. Raizada, and R.K. Varshney, "Modelling a Fiber Half-block with Multimode Overlay Waveguide," J. Opt. Commun. **17**, 179-83 (1996).
34. G. Raizada, B.P. Pal, and R.K. Varshney, "Estimating performance of fiber optic modulators/switches with multimode electro-optic overlay/interlay waveguide," Opt. Fib. Tech. **2**, 89-97 (1996).
35. R.K. Varshney, "Side-polished fiber coupler half block and devices," in *Guided Wave Optics*, A. Sharma, ed. (Viva Books Pvt. Ltd., New Delhi, India, 2005), pp. 110-121.
36. W. Johnstone, "Side polished evanescently coupled optical fiber overlay devices: a review," in *Guided wave optical components and devices: basics, technology and applications*, B.P. Pal., ed. (Academic Press, Elsevier, Burlington, 2006), pp. 225-232.
37. R.K. Varshney, A. Singh, K. Pande, and B.P. Pal, "Side-polished fiber-based gain-flattening filter for erbium doped fiber amplifiers," Opt. Commun. **271**, 441- 444 (2007).
38. B.P. Pal, "All-fiber guided wave components," in *Electromagnetic fields in unconventional structures and materials*, A. Lakhtakia and O.N. Singh**,** eds. (John Wiley, New York, 2000), pp. 359-432.
39. K. T. Kim, S. Hwangbo, J. P. Mah, and K. R. Sohn, "Widely tunable filter based on coupling between a side-polished fiber and a tapered planar waveguide," IEEE Photon. Technol. Lett. **17**, 142–144 (2005).
40. A. Sharma, J. Kompella, and P.K. Mishra, "Analysis of fiber directional couplers and coupler half-blocks using a new simple model for single-mode fibers**,"** IEEE J. Lightwave Technol. **8**, 143-151 (1990).
41. A.K. Ghatak, K. Thyagarajan, and M.R. Shenoy, "Numerical analysis of planar optical waveguides using matrix approach," IEEE J. Lightwave Technol. **5**, 660-667 (1987).

#86448 - $15.00 USD Received 13 Aug 2007; revised 24 Sep 2007; accepted 24 Sep 2007; published 1 Oct 2007

42. M.J.F. Digonnet, J.R. Feth, L.F. Stokes, and H.J. Shaw, "Measurement of the core proximity in polished fiber substrates and couplers," Opt. Lett. **10**, 463-465 (1985).

1. Introduction

Dense wavelength division multiplexed (DWDM) optical transmission systems require high output power, low noise figure erbium doped fiber amplifiers (EDFA's) with a high level of gain flatness over a wide and well-managed bandwidth [1]. Complexity of modern DWDM systems also require that under dynamic operating conditions like add/drop of signals, the EDFA's maintain gain flatness across their gain spectra so that approximately equal power levels are maintained for different signal channels at their output. Unfortunately the gain spectrum of a typical EDFA is characterized with a non-uniform gain spectrum, which unless compensated/controlled may induce bit-error rate (BER) for some of the DWDM channels to increase beyond acceptable limits due to differential optical signal to noise ratio (OSNR) and reduce the usable bandwidth of the amplifiers in a cascaded chain of EDFA's [1]. Moreover, the non-uniform gain may increase the amplified spontaneous emission (ASE) power that could self-saturate an EDFA and reduce the pumping efficiency. In the literature several approaches have been proposed to achieve flat gain bandwidth of EDFA's. One of the approaches has been to add certain amount of Al_2O_3 and P_2O_5 during the process of fabrication of the erbium-doped fiber itself [2, 3] or use tellurite-based host glass for Er^{3+} doping [4-6]. Other examples of alternative approaches involved use of discrete gain equalizing or gain-flattening optical filters such as the Mach-Zehnder (MZ) optical filter [7], the acousto-optic filter (AOF) [8,9], the fiber-loop mirror (FLM) filter [10,11], variable optical attenuator-based filter [12], fiber Bragg grating [13-15] and the long period fiber grating (LPFG) filters [16-24]. MZ and fiber grating-based filters are expensive and usually require additional compensation means for their temperature sensitivity while AOF's require complicated electrical signal processing, and FLM's typically involve relatively high insertion loss. Majority of these gain-flattening filters work for fixed operating conditions or usually require complex procedures to tune their filter characteristics to meet demands of dynamic situations like add/ drop of wavelength channels, variation in the channel input powers or change in pump powers. Therefore, it is often desirable that practical GFF's/ GEF's should possess features like flexible tunability.

An alternative all-fiber technology platform for realizing wavelength filters exists, which exploits side-polished fiber (SPF) half-coupler blocks [25-36]. Functionally, these SPF-half coupler-based filters rely on resonance between the mode effective indices of the SPF-coupler and one of the MMOW high order modes close to its cut-off and hence, were naturally designed to achieve narrowband channel drop or pass band filters for the wavelength(s) at which this resonance occurs. Almost every reported filters based on this physical principle, were focused on searching for the resonance wavelength(s) at the design stage followed by experimental confirmation of the same through measurement of the filter's transmittance as a function of wavelength, in which resonance could be easily identified from the position of the notch (i.e. dip) in the transmittance curve. Scarcely, there were reports in the literature about modeling shape of the transmittance curve at resonance. In view of this, the SPF-half coupler technology platform was rarely exploited to realize GFF/GEF's, which require a relatively wide broad-shaped band-stop filter characteristic such that its transmittance versus wavelength curve inversely matches the broad non-uniform portion of the gain spectrum of an EDFA centered around a wavelength ~ 1530 nm. Recently, a GFF has been reported using a SPF-half coupler loaded with a uniformly thick multimode overlay waveguide (MMOW) [37]. Such SPF-MMOW configurations were indeed extensively used to realize various all-fiber devices like modulators, switches, polarizers etc as they provide many attractive features such as low insertion loss, low back reflections, and good mechanical reliability [35, 36, 38]. In [37], it was shown that the resonance wavelength (notch position) and the peak loss at

#86448 - $15.00 USD Received 13 Aug 2007; revised 24 Sep 2007; accepted 24 Sep 2007; published 1 Oct 2007

resonance (notch depth) of such GFF's could be tailored to the desired values by appropriately choosing the MMOW thickness and refractive index. However, in practice, choosing MMOW with appropriate refractive index and thickness afresh every time is quite cumbersome.

In this paper, we demonstrate for the first time, to the best of our knowledge, tunable gain equalization of DWDM signals within the C-band of an EDFA under varying operating conditions through a GEF device that exploited the SPF half-coupler technology platform. The loss spectrum of the GEF device is tuned through mechanical displacement of the SPF half-coupler relative to a tapered MMOW. Optimized values of the optogeometric parameters of the device were obtained through a semi-numerical normal mode analysis [37], which proved to be a simple and very useful tool to model and design the SPF half-coupler-based devices. We may mention here that a recent report on realization of a tunable narrow-band SPF coupler-based filter involving use of a tapered MMOW that appeared in the literature [39] *differs* from ours as it exploited tunability through relative movement in the *transverse* direction and its design/model relied only on searching for resonance dip (and tunability of its depth) with no mention of design of either the overall transmittance curve centered at the location of the notch or control of the width of the notch.

2. Functional principle of the GEF

Schematic diagram of the SPF-tapered MMOW-based gain flattening filter (GFF) is shown in Fig. 1(a). The GEF device is realized by evanescently coupling the SPF to a tapered MMOW

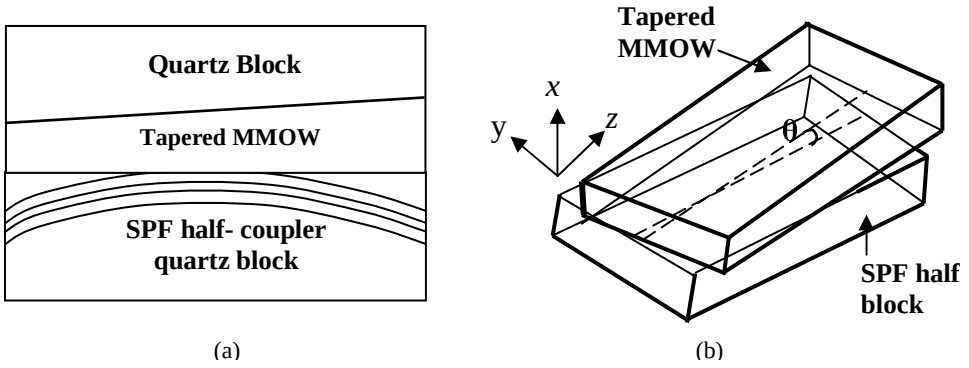

Fig. 1. Schematic diagram of (a) SPF loaded with tapered MMOW (b) position of SPF half block relative to tapered MMOW.

placed overhead. The underlying physical principle is based on phase matching, i.e., resonance between the effective index, n_{ef} ($n_{cl} < n_{ef} < n_c$, where n_c and n_{cl} are the core and cladding refractive indices of the fiber, respectively) of the SPF mode, and the effective index (n_{eo}) of the highest order mode of the MMOW. Since n_{ef} of the guided mode in a typical single-mode fiber (SMF) is just a little greater than its cladding index, it is likely to closely match that of the highest-order mode of the asymmetric MMOW having remaining SPF cladding as its substrate (and silica block as superstrate). Effective index matching (i.e. resonance) can be achieved by tuning any of the MMOW parameters (its refractive index, thickness) or input wavelength, which results in resonant transfer of the power from the fiber to the MMOW. Since the MMOW is highly dispersive, meaning thereby that effective indices of the overlay waveguide are strongly wavelength dependent, the transmitted power would exhibit an almost periodic variation (i.e. periodic notches) with increase in wavelength. This occurs due to sequential phase resonance with subsequent lower order modes of the MMOW (because its previous highest order mode goes in to cut off with increase in

#86448 - $15.00 USD Received 13 Aug 2007; revised 24 Sep 2007; accepted 24 Sep 2007; published 1 Oct 2007

wavelength) if the interaction length between the SPF and the MMOW were sufficiently long. The location of the resonant wavelengths and spacing between them depend on the nature of phase matching and extent of interaction between the guided mode of the SPF and those of the MMOW.

For our device, *firstly* the phase matching wavelength is required to coincide with the gain peak wavelength of the EDFA (typically ~ 1530 nm) and *secondly*, the spacing of the next resonance should be ~ 40 nm further away from that resonance. These parameters were tailored to the desired values through our model by adjusting the geometric parameters of the polished fiber and MMOW parameters. The notch depth and full width at half-maximum (FWHM) of the notch depend on the strength of coupling between the SPF half-coupler and the MMOW. The coupling strength depends on the waveguide separation, radius of curvature of the fiber, and optogeometric parameters of the MMOW and the SPF [34, 35]. The targeted FWHM of the filter notch should be ~ 10 nm, whereas peak loss should match the inverse height of the EDFA gain peak, which can vary between 6 ~ 8 dB for most EDFA's. By appropriately choosing the MMOW and SPF parameters, the loss spectrum of the GEF was tailored to flatten the gain spectrum of the EDFA under test. However, the tunability of the device could be achieved solely through the tapered nature of the MMOW. Figure 1(b) illustrates schematics of the relative position of the SPF half block and the tapered MMOW. Here, *z* and *y* directions are along the longitudinal (i.e., slot length) and transverse directions, respectively, and θ is the tilt angle. The SPF half block was moved in the *yz*-plane to tune the loss spectrum of the device. It is important to mention that the movement in *z*-direction mainly causes tuning of the notch position, while the tuning of the notch depth was achieved through combination of translational movements along *y*- and *z*-directions and control of the tilt angle θ.

3. Modeling of the device

Our basic device structure consists of a planar MMOW, which is evanescently coupled to a SPF half-coupler having a limited cladding on one side, as shown in Fig. 1(a). The device response of such a structure can be described through variation in fractional throughput power P_f (= P_{out}/P_{in}, where P_{in} and P_{out} are the powers at the input and output ends, respectively, of the fiber) across the SPF as a function of the input wavelength (λ) or overlay refractive index (n_o). Functionally, these devices behave in a manner similar to an asymmetric directional coupler. To model the device, we have used a semi-numerical normal mode analysis, which is simple and quite general to model all such SPF-to-MMOW evanescent coupler devices. The normal mode formalism involves two steps: in step 1, the SPF was replaced by an equivalent planar guide (EPG) [40] and in step 2, a simple matrix method [41] was employed to obtain the normal modes of the resultant one-dimensional multi-layer structure (MLS). In our theory, we have taken into account the curvature of the fiber-lay by using a staircase approximation [37] to evaluate the transmittance of the composite device. The actual device, as shown in Fig. 1(a), is now replaced by the structure shown in Fig. 2. If the effective interaction length between the SPF and MMOW is L_{eff}, then the staircase structure comprises of an odd-number of equi-sized (L_{eff}/dz) segments, each of width *dz*, along the direction of propagation *z*. The width of the MMOW and EPG are the same in each segment, whereas the remaining cladding thickness varies as

$$S_i \cong S_0 + \frac{\left|\frac{L_{eff}}{2} - i \times dz\right|^2}{2R_c} \tag{1}$$

where S_i is the waveguide separation in the i^{th} segment, S_0 is the minimum separation between the two waveguides at the center of the block, and R_c is the radius of curvature of the fiber in the groove.

#86448 - $15.00 USD Received 13 Aug 2007; revised 24 Sep 2007; accepted 24 Sep 2007; published 1 Oct 2007

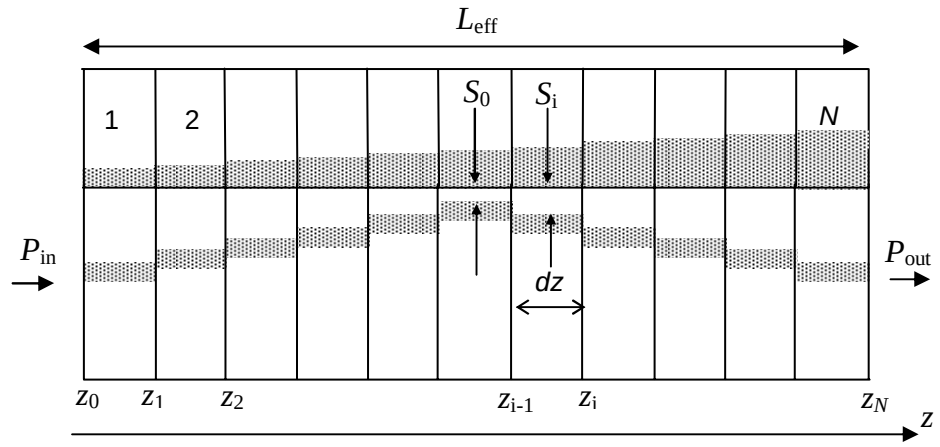

Fig. 2. Diagram illustrating the staircase approximation (for taking into account curvature of the fiber and tapered nature of overlay waveguide) used to model the GEF device (see text).

To evaluate the throughput power, we consider the power exchange between the two waveguides in terms of the normal modes of the planar multi-layer structure consisting of the EPG and MMOW. We assume that unit power is launched into the device through the SPF half-coupler, which would excite all normal modes corresponding to the first segment of the staircase. Since the refractive index distribution corresponding to each segment in the staircase is known, the transverse field distributions of all the normal modes would be known. The excitation coefficients for the modes supported by each successive segment can be obtained in terms of those of the previous ones, and the overlap integrals of the modal fields. Finally, at the output of the device, the total field in the last segment *N* of the staircase would excite the mode of the EPG. So, by calculating the excitation coefficient of this EPG mode, we can obtain the output power and hence the throughput power of the device [33].

4. Fabrication of the device

In order to fabricate the device an initial estimate of the different parameters is required. These parameters, namely, S_0, L_{eff} and R_c were evaluated to be 2 μm, 0.96 mm and 17 cm, respectively. The refractive index and thickness of the MMOW were 1.542 (at the sodium wavelength) and 49.25 μm, respectively. These are the optimized set of parameters to achieve the targeted notch at 1530 nm with the desired FWHM and depth of the notch. In order to fabricate the SPF block, we have used the standard Corning fiber (SMF-28), whose unjacketed portion was fixed into a convex slot cut in a quartz block of length ~ 3 cm, with radius of curvature ~ 17 cm. Then the block was polished up to the desired extent to remove fiber cladding selectively from one side. The throughput power loss of the SPF measured by the well-known liquid drop method was 6.5 dB [42]. In order to yield a tapered MMOW, two spacers of appropriately different thickness were fixed on a second quartz block. The quartz block with polished spacers on its two extreme ends was then placed inverted over the SPF block and the intermediate space between the spacers was filled up with an index matching liquid (IML) of above-mentioned refractive index; this step yielded a tapered MMOW with the IML forming its core.

5. Results and discussion

Detailed numerical investigations were carried out for optimization of the device parameters and to show the tunability of the loss spectrum of the device. To demonstrate the tunability of

#86448 - $15.00 USD Received 13 Aug 2007; revised 24 Sep 2007; accepted 24 Sep 2007; published 1 Oct 2007

(a)

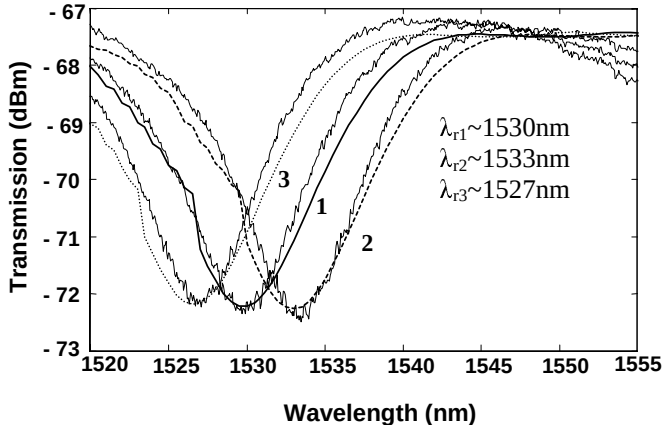

(b)

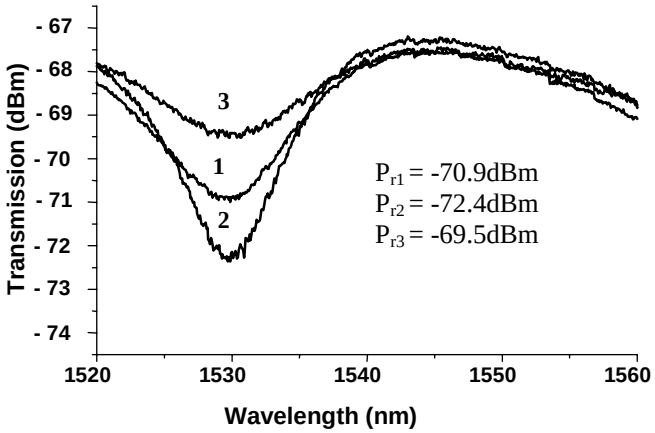

Fig. 3. Three sample results to demonstrate tunability of transfer function of the device through controlled translation of SPF half-coupler block relative to the tapered MMOW; (a) tuning of the notch position (b) tuning of the notch depth.

the device experimentally, the fabricated device was mounted over a standard motorized rotational stage attached with *x*-*y* translation stage (Newport Corporation, USA) and light from a broadband source was launched at the input. The output power was measured by using an optical spectrum analyzer (OSA, HP70951B) having a wavelength resolution bandwidth of 0.05nm. The SPF half-coupler and the tapered MMOW were moved relative to each other to achieve tuning of the notch position and its depth. Figure 3(a) shows both the theoretical and the experimental results with respect to shift in the resonance wavelength when SPF half-coupler and tapered MMOW were moved relative to each other. It clearly indicates the good agreement between our model and the experimental results.

Here, curve-1 corresponds to central position (i.e., $z = 0$, $y = 0$ and $\theta = 0$), whereas curves-2 and 3 correspond to $z \cong -0.15$ mm and 0.15 mm, respectively, while there is no change in values of y and θ. Resonance wavelengths for curves-1, 2 and 3 were ~ 1530 nm, ~1533 nm and ~1527 nm, respectively. It is clear from this figure that by introducing a total displacement of just 0.30 mm along the groove length, the resonance position can be tuned through ~ 6 nm. We may mention that the tuning range of the resonance position is determined principally by the refractive index and the effective thickness of the MMOW. In our case (with the refractive index of the MMOW as 1.542 at the sodium wavelength) and for notch depth of ~ 5 dB fixed at ~ 1530 nm, we have observed that the notch position can be

#86448 - $15.00 USD Received 13 Aug 2007; revised 24 Sep 2007; accepted 24 Sep 2007; published 1 Oct 2007

varied over a broad range of ~ 20 nm from ~ 1525 nm to 1545 nm through translational shift of the SPF half-coupler relative to the tapered MMOW. The tuning of the notch depth is shown in Fig. 3(b). In this case again, curve-1 corresponds to central position (i.e., z = 0, y = 0 and θ = 0), whereas curves-2 and 3 correspond to z = 1.42 mm, y = 0.02 mm, $\theta = 0.31^0$ and z = -1.41 mm, y = -0.43 mm, $\theta = -0.73^0$, respectively. The notch depth for curves-1, 2 and 3 were approximately -70.9 dBm, - 72.4 dBm and -69.5 dBm, respectively. We may mention that although this figure shows a tuning of the notch depth by ~ 3 dBm, we have observed that the notch depth can be easily varied over a range of ~ 4 dBm through this technique. Thus, Figs. 3(a) and 3(b) clearly demonstrate that depth and position of resonance can be tuned over a large range by our proposed tuning technique.

To demonstrate the gain equalization performance of the fabricated SPF-tapered MMOW device, detailed experimental studies were carried out under varying operating conditions. The GEF was spliced with a 13-m long EDF having peak absorption coefficient of 6±1 dB/m at 1530 nm. The EDF was forward pumped with a 980 nm laser diode. Then eight DWDM signals (ILX Lightwave System model No. 7900B), which were distributed over the wavelength range of 1529 -1559 nm, were fed from a C-band standard DFB laser source. Initially, the EDF was pumped with a pump power of 140 mW and the signal powers in all the eight signals were kept at -20 dBm. Figure 4(a) shows the measured output spectra of the

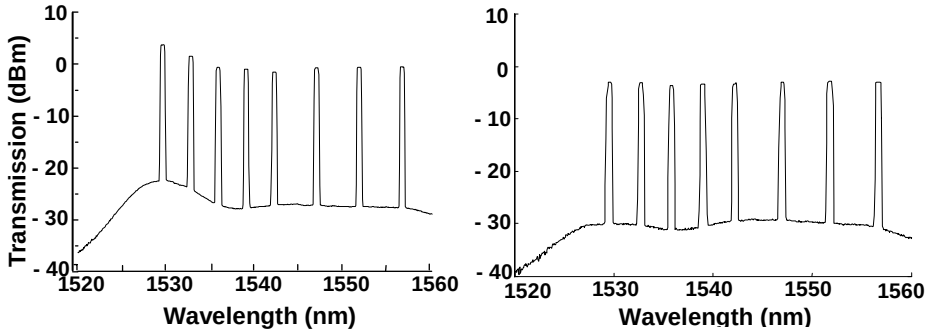

Fig. 4. Measured signal output spectra for 8 amplified DWDM signal channels from the EDFA in an OSA (a) without and (b) with the GEF integrated with the EDFA; signal power was –20 dBm and pump power was 140 mW.

EDFA without the GEF. The peak-to-peak power variation among the amplified channels was 5.2 dB. After introducing the fabricated SPF-MMOW-based GEF device having relative position z = 2.451 mm, y = 0.085 mm, θ = 0, we measured the gain spectrum of the EDFA again. Measured spectrum is shown in Fig. 4(b). We may mention that all these numerical values for the relative positions were with respect to the central position of Fig. 3(a). This figure shows that peak-to-peak power variation amongst the amplified signals has dropped dramatically to within ±0.35 dB (shown more explicitly in Fig. 7 later).

It is well known that the shape of the gain spectrum of an EDFA varies with the changes in pump and/or signal powers [1]. Accordingly, we have also studied performance of the GEF in conjunction with the EDFA for different pump and signal powers. Figure 5(a) depicts equalization maintenance of the output signal powers when input signal power level was varied from -20 dBm to -15 dBm while the pump power was kept fixed at 140 mW with the device having relative position z = 4.11 mm, y = 2.18 mm, θ = 0. In the subsequent experiment the pump power was reduced from 140 mW to 85 mW keeping signal power level fixed at -20 dBm; corresponding measured equalization of signal powers is shown in Fig. 5(b). In this case relative position of the device was z = 1.91 mm, y = 3.85 mm, θ = 0. Without

#86448 - $15.00 USD Received 13 Aug 2007; revised 24 Sep 2007; accepted 24 Sep 2007; published 1 Oct 2007

integration of the GEF device in the layout of the EDFA, in either of the above cases such variations in the operating conditions would have significantly deteriorated the gain flattening characteristics of the EDFA. The output power levels were equalized to within ±0.35 dB (shown more explicitly in Fig. 7 later) in both the cases through translation of SPF half-coupler relative to the tapered MMOW in the *yz*-plane.

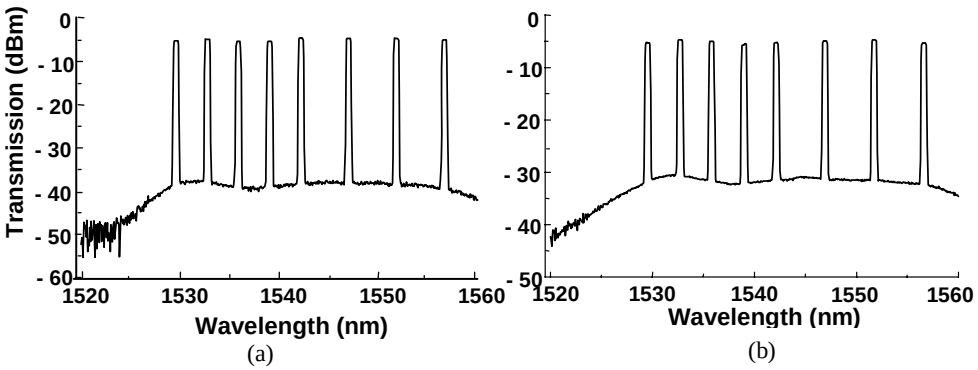

Fig. 5. (a) Equalized signal output spectra from the EDFA in the presence of eight DWDM signal channels when signal power was changed from –20 dBm to –15 dBm; pump power was kept fixed at 140 mW; (b) Corresponding results when the pump power was reduced from 140 mW to 85 mW; input signal power level was kept at –20 dBm.

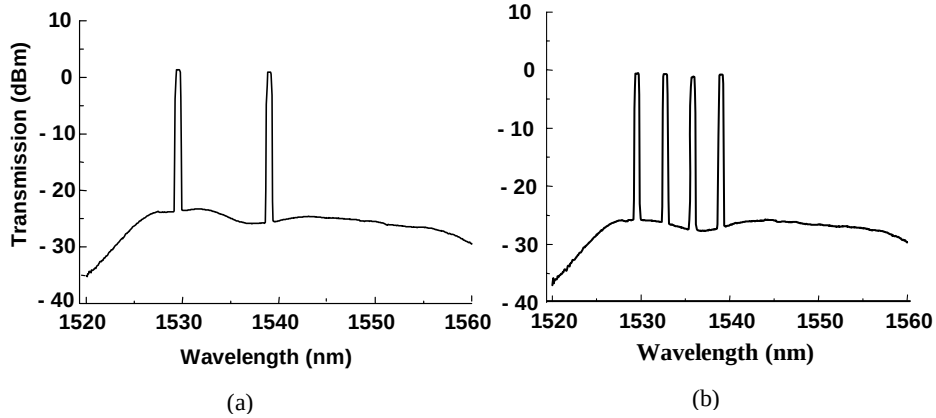

Fig. 6. Equalized signal output spectra from the EDFA; for case (a) 6 DWDM channels were dropped and for case (b) two channels were added.

Another important oft-quoted situation in a dynamic DWDM transmission scenario, which could cause significant variations in the gain spectrum of an EDFA, is when a channel(s) is (are) added or dropped from the DWDM stream. Figure 6 (a) shows the gain equalization amongst different channels when six out of eight channels were dropped. For this case, relative position of the device was $z = 0.012$ mm, $y = 0$, $\theta = 0$. In this case, the gain spectrum was seen to have flattened within ±0.25 dB, which was even better than the previous result. In the next experiment we added two channels (i.e., total number of input signals were now four) to test the performance of the GEF device when channels were added. Equalized output spectrum of the EDFA with those 4 signal channels is shown in Fig. 6 (b). In this case, relative position of the device was $z = 0.095$ mm, $y = 0.006$ mm, $\theta = 0$. It is evident that in this case the GEF device has resulted in power equalization within ±0.30 dB within the gain bandwidth of the EDFA.

In order to demonstrate performance of the proposed GEF device under varied operating conditions more explicitly, maximum peak-to-peak power variations, for all the gain

#86448 - $15.00 USD Received 13 Aug 2007; revised 24 Sep 2007; accepted 24 Sep 2007; published 1 Oct 2007

flattening results mentioned above, are depicted in Fig.7. Here, the average peak power level was set to zero for each case. This clearly shows that peak-to-peak power variation is well within ± 0.35 dB for all the cases and in some specific cases ≤ ±0.25 dB. We may mention that the gain equalization within ±0.35 dB over a wavelength range of 30 nm under varying operating conditions that has been achieved through our fabricated GEF device is comparable or even better than the earlier reported results for other GFFs e.g., in case of acousto-optic filters, it was within ± 0.35 dB [8], that of FLM-based filters it was within ± 0.5 dB [11], while for LPFG-based filters it was within ± 0.35 dB [21]. The polarization dependent loss (PDL) of the fabricated GEF device was also measured with a photonics analyzer (Adaptif-2000, GmBH, Germany make) and it was found to be < 0.4 dB across the entire C-band. This indicates the low polarization dependence of the device. We may mention that although the proposed GEF device exhibited, in general, level of equalization of the gain spectrum similar to acousto-optic filters and LPFG-based filters, this device has all the advantages of side-polished fiber device features like low insertion loss, good mechanical stability, easy integration, and tunability. We have also studied fabrication tolerances on different

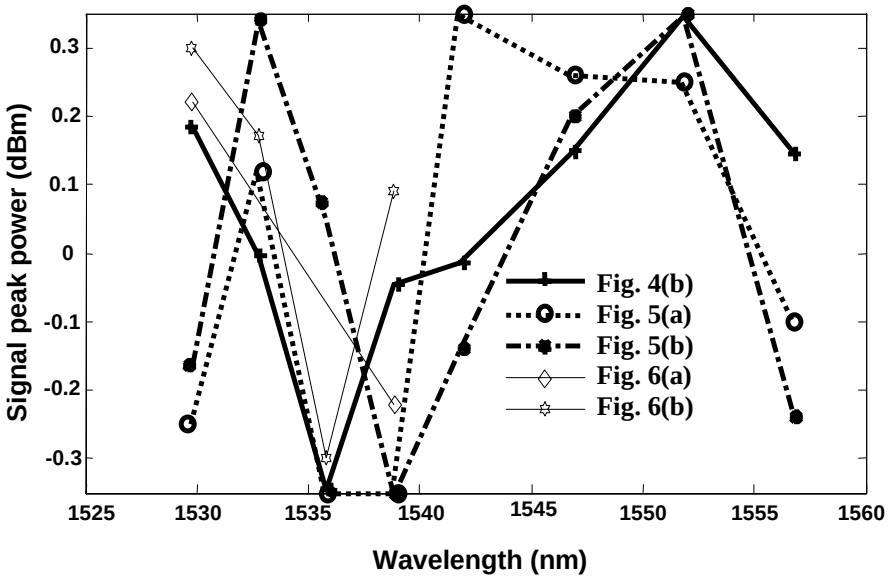

Fig. 7. Variation of peak signal power with respect to the average gain for all the gain flattening results shown above (average power level is set to zero for each case).

parameters with regard to performance of the GEF device reported here. Performance tolerance to variations in characteristic parameters S_0 (remaining cladding thickness) and R_c (radius of curvature of the convex slot on the substrate silica block) were studied theoretically. Figure 8(a) shows estimated variation in P_f vs. λ of such a GEF device for different cases; the solid curve in the figure corresponds to the optimum value of S_0 while the dashed and the dotted curves correspond to the variation in S_0 by -2% and +2%, respectively, from its optimum value. Similarly, Fig. 8(b) illustrates the variation in the throughput power spectrum for the three cases namely, for optimum value of R_c (solid curve) and when R_c is varied by ±10 % (dotted and dashed curves, respectively). From these results it can be inferred that S_0 is required to be controlled to a greater degree of precision relative to what is required for the other fabrication parameter R_c.

#86448 - $15.00 USD Received 13 Aug 2007; revised 24 Sep 2007; accepted 24 Sep 2007; published 1 Oct 2007

(a)

(b)

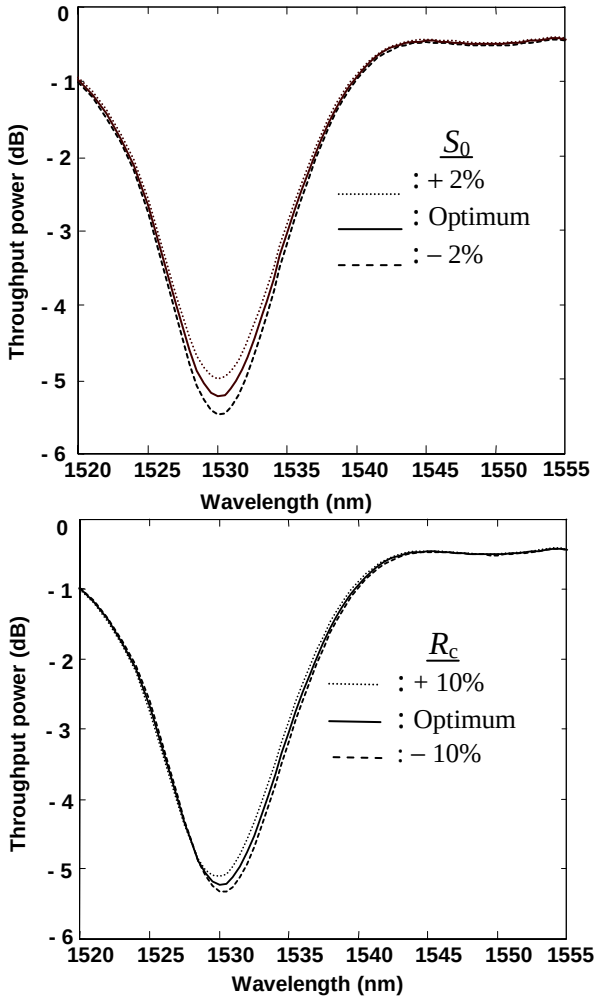

Fig. 8. (a) Various curves showing the variations in throughput power spectra for ±2% variations in the parameter S_0 from its optimum value; (b) Corresponding curves for ±10% variations in the parameter R_c.

6. Conclusion

We have theoretically modeled, designed, and experimentally demonstrated a simple and easily realizable all-fiber tunable notch filter for gain equalization of EDFA. A semi-numerical normal mode analysis along with a staircase approximation was used for optimization of the device parameters at the design stage. The device was realized by loading a SPF half-coupler block with a tapered MMOW. Displacement of the SPF block relative to the tapered MMOW was exploited to tune the transmission characteristics of the fabricated GEF. The gain equalization between DWDM signal channels well within ±0.35 dB or even less over a bandwidth of 30 nm in the C-band of the EDFA under varied operating conditions, which included add/drop of signals was demonstrated. This evanescently coupled all-fiber device was fabricated from standard communication fiber (SMF-28), and hence this GEF device could be easily spliced to the transmission fiber in a DWDM fiber link with negligible splice loss. Tolerances on various fabrication parameters of the device were also reported.

#86448 - $15.00 USD Received 13 Aug 2007; revised 24 Sep 2007; accepted 24 Sep 2007; published 1 Oct 2007

Acknowledgements

The authors would like to thank Prof. K. Thyagarajan and Prof. M. R. Shenoy for fruitful discussions and Mr. Umesh Tewari for his help in the measurements. One of the authors (BPP) thanks Corning Inc. for supply of SMF-28 fiber for our internal research and students training. This work was partially supported by the Department of Science and Technology, Govt. of India.

#86448 - $15.00 USD Received 13 Aug 2007; revised 24 Sep 2007; accepted 24 Sep 2007; published 1 Oct 2007